



Manganese-enhanced MRI to evaluate neurodegenerative changes in a rat model of kainic acid-induced excitotoxicity

Melda Apaydın, Vedat Evren, Oytun Erbaş, Cem Çallı, Gönül O. Peker, Dilek Taşkıran

PURPOSE

Manganese-enhanced magnetic resonance imaging (MEMRI) has been used to detect brain activity based on the ability of active neurons to take up manganese ions through calcium channels. Kainic acid (KA), an analog of excitotoxic glutamate, can elicit selective neuronal death in the brains of rodents, of which the pathological changes partially mimic neurodegeneration in the central nervous system. We used *in vivo* MEMRI to evaluate neurodegenerative changes in an excitotoxicity model induced by KA in rats.

MATERIALS AND METHODS

Adult Sprague-Dawley rats (220–250 g) were injected with either KA or saline into the right lateral ventricle. Precontrast and postcontrast MEMRI sessions were obtained. Region of interest (ROI) analyses were performed on both injected (saline and KA) and contralateral (normal) sites in the hippocampal area. All brains were evaluated histologically following MEMRI.

RESULTS

Analysis of percentage change in ROI intensities of T1-weighted fluid-attenuated inversion-recovery MR images in the hippocampal area revealed a significant difference between the KA-injected (ipsilateral) and contralateral sites ($P = 0.008$), whereas no significant difference was observed between the saline-injected and contralateral sites. Furthermore, there was a significant difference between ipsilateral sites of the saline-treated and KA-treated groups ($P = 0.026$). The histological results supported these findings.

CONCLUSION

MEMRI is a simple and useful *in vivo* method for detecting neurodegenerative changes due to excitotoxicity in the rat brain. The development of a manganese-based contrast agent that can be safely used in humans is warranted to investigate neurological disorders.

Manganese (Mn^{2+}) is an essential metallic element in cell biology. Free radical detoxification, neurotransmitter synthesis, and electron transport are some of the biological functions of this element (1). Mn^{2+} , as a calcium (Ca^{2+}) analog, uses the same transport system and enters neurons and other excitable cells through voltage-gated Ca^{2+} channels. By replacing Ca^{2+} with Mn^{2+} , it is possible to produce intracellular accumulation of Mn^{2+} in neurons undergoing cell death. Consequently, Mn^{2+} is transported along neural axons, making Mn^{2+} an appropriate contrast agent in magnetic resonance imaging (MRI) studies of the central nervous system (CNS) and neural pathways (2). Mn^{2+} reduces the T1 relaxation time and increases tissue contrast in T1-weighted images (3). Recently, it has been suggested that Mn^{2+} -enhanced MRI (MEMRI) can be used as an *in vivo* method to investigate the morphological and functional changes in the central and peripheral nervous systems in animals (1–3).

Excitotoxicity is considered an important cause of neurodegenerative disease. Kainic acid (KA), an epileptogenic and neuro-excitotoxic agent, is widely used for inducing neurodegeneration in animal studies (4–6). It is a specific agonist for kainate receptors, which are ionotropic glutamatergic receptors that modulate transmission and excitability. KA has been used for modeling of epilepsy because of its strong stimulatory effects (4–7).

MRI, which does not require animals to be sacrificed, is an exceptional tool for longitudinal *in vivo* CNS studies (8). In the present study, we employed *in vivo* MEMRI to evaluate neurodegenerative changes in an excitotoxicity model induced by KA in rats. In addition, histological (Timm's staining) and immunohistochemical (Bax) analyses were performed to confirm neurotoxicity following KA administration.

Materials and methods

Animals

Ten adult Sprague-Dawley rats (220–250 g) were housed in cages and maintained under standard conditions with 12 hours light/dark cycles at room temperature ($22\pm 2^\circ C$). The rats were fed a standard pellet diet and tap water *ad libitum* for the duration of the study. The experimental procedures were performed according to the guidelines of the local Institutional Animal Care and Ethical Committee of Ege University (approval code: 2011-102). All chemicals were obtained from Sigma-Aldrich Inc. (St. Louis, Missouri, USA) unless otherwise noted.

Kainic acid treatments

KA was prepared as a stock solution at 1 mg/mL in sterile phosphate-buffered saline (PBS). Rats were deeply anesthetized using a

From the Department of Radiology (M.A. ✉ meldapaydin@gmail.com), İzmir Katip Çelebi University Atatürk Education and Training Hospital, İzmir, Turkey; the Departments of Physiology (M.A., V.E., O.E., G.O.P., D.T.) and Radiology (C.Ç.), Ege University School of Medicine, İzmir, Turkey.

Received 27 December 2012; revision requested 19 January 2013; revision received 19 March 2013; accepted 21 March 2013.

Published online 25 July 2013.
DOI 10.5152/dir.2013.200

mixture of ketamine hydrochloride (40 mg/kg; Alfaxone[®], Alfasan International B.V., Woerden, Holland) and xylazine hydrochloride (4 mg/kg; Alfaxone[®], Alfasan International B.V.) intraperitoneally (i.p.), and then were placed in a stereotaxic frame. The fur over the animal's head was shaved using an electric clipper. The scalp was cleaned with a 10% betadine solution, and a 1 mm incision was made to expose the bregma. A hole was drilled for intracerebroventricular (i.c.v.) administration of KA (Fig. 1). KA was dissolved in saline (0.5 $\mu\text{g}/\mu\text{L}$; $n=5$), and 1 μL was slowly infused (0.2 $\mu\text{L}/\text{min}$) unilaterally into the right lateral ventricle using a 28-gauge needle attached to a 10 μL Hamilton syringe (7, 9). The coordinates for the KA infusion were applied according to the rat brain atlas of Paxinos and Watson (10) as follows: anteroposterior, 1.2 mm; lateral, 2 mm; vertical, 3.6 mm. The sham-operated animals ($n=5$) received isotonic saline only. The needle was left in place for an additional 5 min for complete diffusion of the drug. All animals were administered 1 mL isotonic saline subcutaneously following surgery to aid recovery. They were housed two to three per cage and monitored daily for behavior and health conditions.

Mn²⁺ injection and MEMRI sessions

After a recovery period of 10 days, MRI sessions were performed on day 10 (precontrast) and day 12 (postcontrast). Before the MRI experiments, animals were anesthetized as in the experimental protocol with a single intraperitoneal dose of anesthesia. The systemic Mn^{2+} injection (40 mg/kg in saline; MnCl_2 , Sigma-Aldrich Inc.) was performed i.p. 24 hours before the imaging (3). All images were acquired using a 3 Tesla (T) MR scanner (Magnetom Verio, Siemens Healthcare, Erlangen, Germany) and an eight-channel wrist coil resonator (Siemens Healthcare). The optimum flip angle and time for repetition (TR) were chosen for adequate T1 enhancement due to Mn^{2+} as well as a short time to echo (TE) for compensation of T2-weighted signal loss. Data acquisition: coronal fluid-attenuated inversion-recovery (FLAIR) (TR/TE/time for inversion [TI], 2040/11/873.8 ms; field of view, 50);



Figure 1. Preparation of the animal's head for stereotaxic administration of kainic acid.

number of excitations (NEX), 8; number of slices, 8; slice thickness, 1 mm; gap, 0.1 mm; flip angle, 150°; resolution, 128 \times 128; voxel, 0.4 \times 0.4 \times 1 mm; SNR, 1; bandwidth, 260 Hz/Px. The MEMRI scanning time was 20 min/animal. The average T1 FLAIR values (pixel count, 4 and 5) of the selected slices were calculated from the regions of interest (ROIs). ROI analyses were performed on both injected (ipsilateral) and contralateral sites of rats treated with KA and saline (11).

Bax immunohistochemistry

Apoptotic cell death was assessed by Bax immunohistochemistry. Briefly, all animals were anesthetized via i.p. injection of ketamine (40 mg/kg)/xylazine (4 mg/kg) and perfused with 200 mL 4% paraformaldehyde in 0.1 M PBS. After the brains were removed, they were transferred to 30% sucrose and stored at 4°C until infiltration was complete. The brains were cut coronally on a frozen sliding microtome at 40 μm and mounted on gelatinized glass slides. Next, sections were incubated with H_2O_2 (10%) for 30 min to eliminate endogenous peroxidase activity, and then were blocked with 10% normal goat serum (Invitrogen, Life Technologies Co., Carlsbad, California, USA) for 1 hour at room temperature. Thereafter, sections were incu-

bated in primary antibody against Bax (1/100; Santa Cruz Biotechnology Inc. Santa Cruz, Dallas, Texas, USA) for 24 hours at 4°C. Antibody detection was performed using the Histostain-Plus Bulk kit (Invitrogen, Life Technologies Co.) against rabbit IgG, and 3,3'-diaminobenzidine was used to visualize the final product. All sections were washed in PBS and photographed using an Olympus C-5050 digital camera mounted on an Olympus BX51 microscope (Olympus, Tokyo, Japan). Immunoreactivity in the brain sections was quantified by measuring the intensity per area using ImageJ software (National Institutes of Health, Bethesda, Maryland, USA). The intensity measurements were performed in five sections for each animal ($n=4$) and 6–8 microscopic fields in each section (12).

Timm's staining

Timm's sulfide silver method was used to clarify the MRI changes in rats following KA injection. Timm's staining is a semi-quantitative autometallographic (AMG) histochemical staining technique based on the principles of photography used to trace metals at the cellular level. Synaptic vesicles in glutamatergic axon terminals contain zinc metal, which is either in ionic form or is loosely bound to glutamatergic presynaptic terminals. These

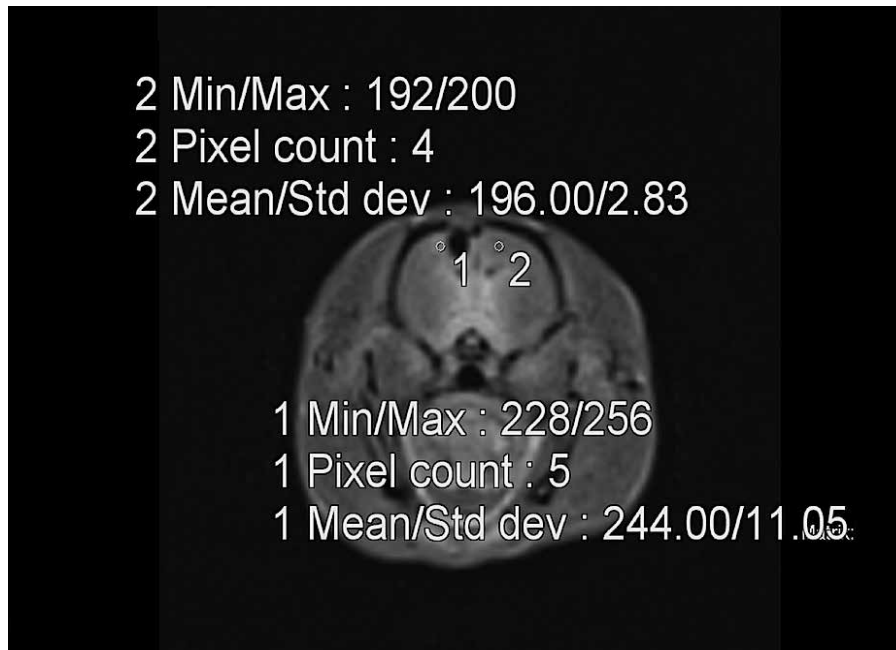


Figure 2. Coronal T1-weighted fluid-attenuated inversion-recovery manganese-enhanced MRI shows region of interest measurements in kainic acid-infused (1) and contralateral (normal) areas (2). Min/Max, minimum/maximum; Std dev, standard deviation.

zinc-containing terminals are termed zinc-enriched terminals. The principle of this histochemical staining is to process the tissue sections with a sulfide-containing solution (sodium sulfide [Na_2S]) during fixation to bind metal ions with sulfide, followed by silver enhancement catalyzed by sulfur. The silver ions precipitate at the site of metals and can be observed as black accumulations (13, 14).

For Timm's staining, the rats were anesthetized and sacrificed by transcardial perfusion with 4% paraformaldehyde followed by 0.37% Na_2S solution. Brains were removed and placed in the same fixative overnight, and then were placed in 30% sucrose solution for cryoprotection. Tissues were frozen and stored at -80°C until sectioning. Cryosections (40 μM) were obtained and placed on gelatin-coated slides. The slides were cleaned, dehydrated, and rehydrated in a series of alcohol and distilled water jars before they were placed in the AMG developer solution. After 75 min, the reaction was stopped by the addition of 5% sodium thiosulfate solution. Slides were placed under running tap water, counterstained with cresyl violet, dehydrated, cleaned, and mounted for microscopic evaluation. The images of the histological slices were captured on a

high-resolution digital camera (Nikon DXM1200, Nikon, Tokyo, Japan) installed in a Nikon microscope (Eclipse E600FN, Nikon). Images were acquired with magnifications of $\times 40$ and $\times 100$.

Timm's staining in the hippocampus (CA3 subregion) was graded from 0 to 5 according to the presence of Timm granules (silver accumulations): 0, no granules at the stratum pyramidale (SP) or stratum oriens (SO); 1, sparse patchy granules at SP or SO; 2, visible granules at SP or SO; 3, prominent granules at SP or SO; 4, continuous prominent granules at SP or SO; 5, band forming and dense granules along CA3 (13, 14).

Statistical analysis

A standard statistical software program was used for analysis. The alterations in signal intensities in ROIs were presented as the percentage change in ROI and calculated by using the formula as follows: Percentage change in ROI = $100 \times ([\text{ROI}_{\text{post}} - \text{ROI}_{\text{pre}}] / \text{ROI}_{\text{pre}})$. The Mann Whitney U test was used to compare signal intensities in ROIs in the hippocampal area between groups and also to compare the quantitative data between saline and KA-treated group for Bax immunohistochemistry. Data were expressed as median (min-max values). *P* value less than 0.05 was deemed to be statistically significant.

Results

On postcontrast MEMRI images in KA-injected rats, hyperintensity was observed in both parts of the globus pallidus, as expected (Fig. 2). Enhancement in the hippocampal area on the KA-injected side was clearly observed. In addition, the analysis percentage change in ROI intensities of T1-weighted FLAIR MR images in the hippocampal area revealed a significant difference between the KA-injected (ipsilateral) and contralateral sites (55.17% [42.36%–115.45%] vs. 17.95% [8.29%–24.48%]; *P* = 0.008) (Figs. 3, 4), whereas no significant difference was observed between the saline-injected and contralateral sites. Furthermore, there was a significant difference between ipsilateral sites of the saline-treated (*n*=5) and KA-treated (*n*=5) groups (55.17% [42.36%–115.45%] vs. 22.10% [46.11%–14.05%]; *P* = 0.026) (Figs. 3, 4).

We performed Bax immunohistochemistry in striatal sections to assess the involvement of apoptotic cell death in KA-induced neuronal injury. The intensity analysis of brain sections displayed a significant enhancement in Bax expression in the KA-treated group (*n*=5) compared to the saline-treated group (*n*=5) (106.3% [96%–116.2%] vs. 92.1% [72%–97.2%]; *P* = 0.016) (Figs. 5, 6).

Timm's staining is an accepted technique for imaging zinc-containing neuronal components. Our observations regarding zinc histochemistry in the hippocampus are in accordance with previous reports (14). We observed prominent mossy fiber sprouting and axonal plasticity in the CA1 and CA3 granule cells of hippocampal sections in the KA-induced group, whereas control animals that received MnCl_2 injection showed no mossy fiber sprouting in histological sections (Fig. 7).

Discussion

Various CNS disorders, including vascular, inflammatory, neoplastic, and neurodegenerative diseases, are frequently investigated in animal models. These models help advance the understanding and treatment options of CNS diseases in humans (15). MRI enables longitudinal, noninvasive neurological studies in experimental animal models without sacrificing the

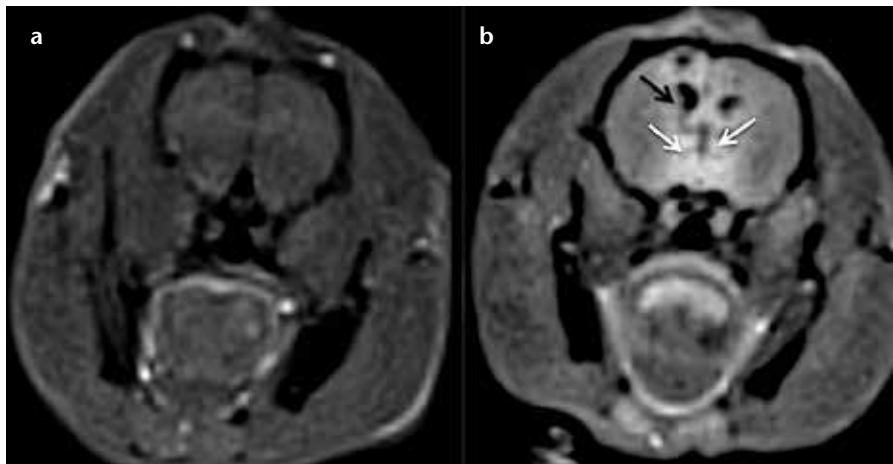


Figure 3. a, b. Representative precontrast (a) and postcontrast (b) coronal, T1-weighted fluid-attenuated inversion-recovery MR images showing bilateral enhancement in the globus pallidus (white arrows) and unilateral enhancement on the kainic acid-injected side in the hippocampal area (black arrow).

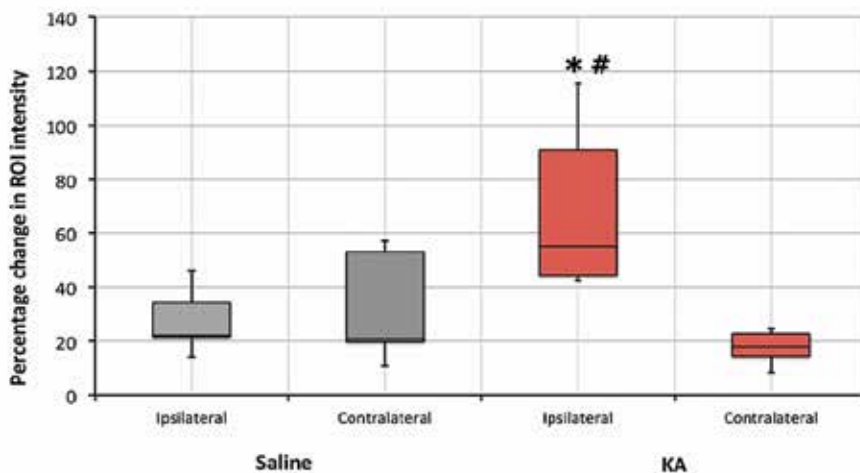


Figure 4. Analysis of percentage changes in region of interest (ROI) intensities revealed a significant difference between ipsilateral and contralateral area in kainic acid (KA) group, whereas no significant difference was observed between the saline-injected and contralateral sites. Also, a significant difference was found between ipsilateral sites of the saline-treated and KA-treated groups. Data are expressed as median with 25th and 75th percentile. Boxes enclose the interquartile range and the median, while whiskers enclose the range (min–max values). * $P = 0.008$ for ipsilateral vs. contralateral sites in KA group, and # $P = 0.026$ for between ipsilateral sites of the saline and KA-treated groups.

animals and provides important anatomical and physiologic information (16). After the first MRI study of a rat reported 30 years ago, the number of studies has increased, particularly in relation to the CNS (15–17).

Excitotoxicity is considered the main mechanism involved in cell death of several CNS diseases, including neurodegenerative disorders. Glutamate, an important excitatory neurotransmitter, causes neuronal damage in various CNS pathologies in excess doses (18). Neuronal damage accompanies Ca^{2+}

influx followed by overproduction of reactive oxygen species and reactive nitrogen species, both of which lead to cell death (4, 18). KA is a glutamate receptor agonist that has been shown to cause excess production of reactive oxygen species, mitochondrial dysfunction and apoptosis in the brain (4, 18). These effects are prominent in hippocampal neurons due to selective vulnerability of AMPA/kainate receptors (4, 18, 19). KA has been found to be 30-fold more effective than glutamate in neurotoxicity in several experimen-

tal studies (20). Intracerebroventricular KA produces brain lesions in rats similar to epilepsy in humans (5). KA-induced status epilepticus is associated with neuronal damage and synaptic reorganization in hippocampal (CA3 and CA1 areas) and limbic structures (20, 21). KA at higher concentrations can also induce excitotoxicity in the medial amygdaloid nuclei (20, 22). Bardgett et al. (23) reported that intracerebroventricular administration of KA produces neuronal loss in limbic-cortical brain regions, which project directly or indirectly to the striatum.

Necrosis has been shown to be the principal lesion following administration of excitotoxic agents; however, apoptotic pathways are also triggered after excitotoxic insult or seizures (24–26). The mitochondrial pathway (intrinsic pathway) of apoptosis begins with the permeabilization of the mitochondrial outer membrane. Several apoptotic signals, including DNA damage, ischemia, excitotoxicity, and oxidative stress, can lead to cell death through mitochondria. The bcl-2 family of proto-oncogenes encodes specific proteins that regulate programmed cell death by either inducing (bax, bid) or inhibiting (bcl-2, bcl-XL) apoptosis under different physiological and pathological conditions. Bcl-2, a cell survival protein, has been observed to be decreased compared to the pro-apoptotic bax, which translocates from the cytosol to the mitochondria during apoptotic cell death (27). Bax promotes apoptosis by inducing mitochondrial membrane depolarization and cytochrome *c* release, whereas bcl-2 inhibits apoptosis by preventing mitochondrial membrane depolarization (28). KA-induced DNA damage has been demonstrated in the mouse hippocampus and neocortex at 24 and 48 hours after intraperitoneal injections. In addition, downregulation of bcl-2 and upregulation of bax has been reported in the same regions of the mouse brain (25). Similarly, Lopez et al. (26) described a slight increase in bax immunoreactivity in the cytoplasm of neurons of the dentate gyrus 24–48 hours after KA injection. They also showed bax translocation to the nucleus in some dying cells in the entorhinal cortex and CA1 area of the hippocam-

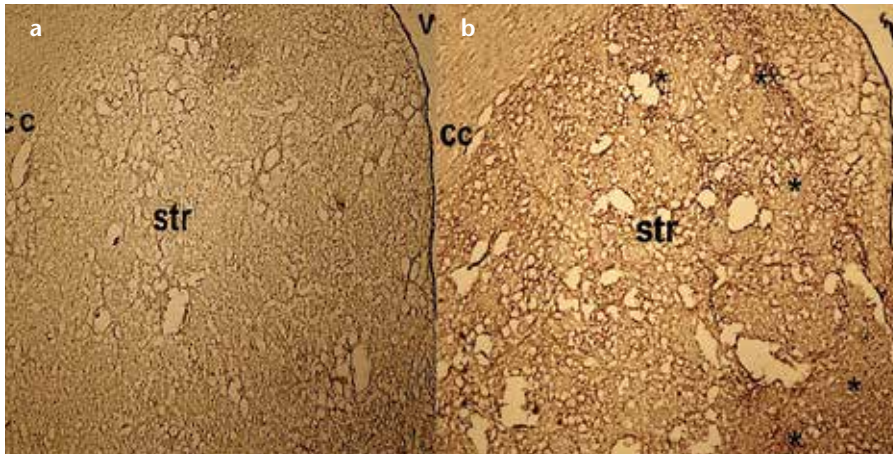


Figure 5. a, b. Bax immunohistochemistry in saline- (a) and kainic acid-infused rats (b). Photos were taken at $\times 40$ magnification. cc, corpus callosum; str, striatum; v, ventricle.

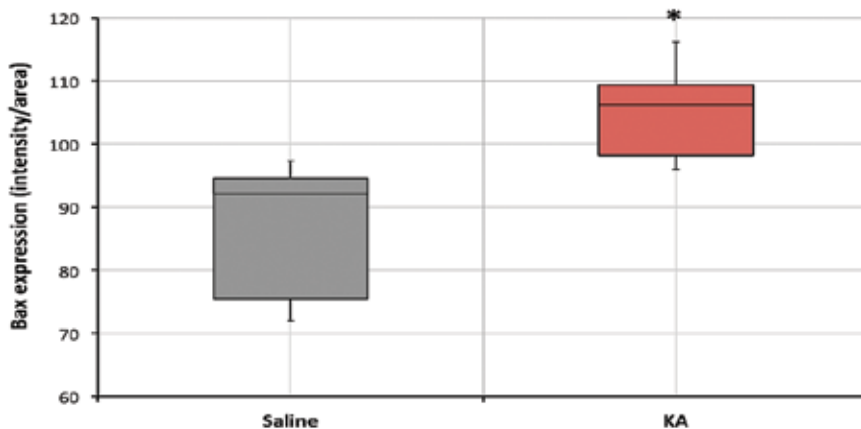


Figure 6. Bax immunoreactivity was significantly higher in kainic acid -treated rats than in saline-treated rats ($P < 0.016$). Data are presented as median (min–max values). Asterisk(*) indicate increased Bax immunoreexpression in the kainic acid-treated group.

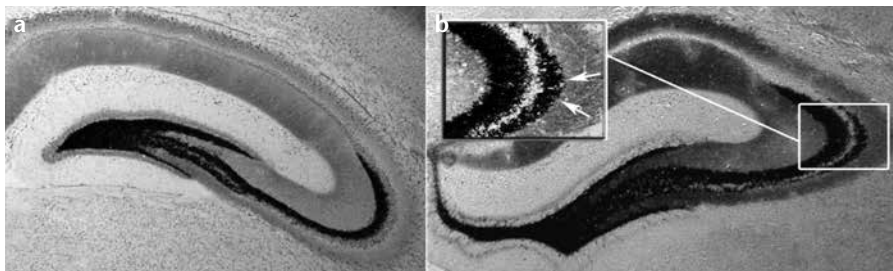


Figure 7. a, b. Histochemical changes in the hippocampal area after kainic acid injection. Timm's staining clearly shows synaptic reorganization and mossy fiber sprouting in the CA3 subregion (inside the square, arrows) in saline- (a) and kainic acid-infused rats (b). Photos were taken at $\times 40$ and $\times 100$ magnifications.

pus following KA administration. In accordance with previous studies, our findings confirm a significant increase in bax immunoreexpression in brain sections of KA-treated rats, indicating the involvement of apoptotic cell death.

Recently, Mn^{2+} has been employed as an exogenous MRI contrast agent to de-

tect neuronal activation, neural architecture, and neuronal connections. In addition to several roles in normal physiology, Mn^{2+} enters excitable cells via Ca^{2+} channels and is transported along neural axons. In the brain, Mn^{2+} accumulates mostly in the globus pallidus, causing hyperintensity on T1-weight-

ed images with a normal T2-weighted signal (14). A dose-dependent signal increase is a biomarker of Mn^{2+} toxicity in the globus pallidus (29).

In the present study, we demonstrated marked Mn^{2+} enhancement on T1-weighted FLAIR images 10 days after stereotaxically induced KA excitotoxicity in rats. There was a prominent enhancement in the globus pallidus. The post-contrast ROI intensities of T1-weighted FLAIR MR images in the hippocampal area were significantly higher in the injured site compared to the contralateral site. In addition, Timm-stained histologic sections showed extensive mossy fiber sprouting in the CA3 subregion, a process that supports new axon collaterals. These findings are consistent with those of previous studies except that our study was conducted using a clinical MR machine that is used in routine practice. For instance, Nairismaği et al. (30) reported enhancement of the MEMRI signal in the dentate gyrus and CA3 subregion of the hippocampus three to five days after injecting $MnCl_2$ into the entorhinal cortex in KA-injected rats. Histological examination of the brains also revealed neuronal loss in the hippocampal subregions in KA-treated rats. Furthermore, severe degenerative changes in other brain areas two weeks following KA injection, including a reduction in the combined thickness of the amygdala and piriform cortex and expansion of the lateral ventricles due to atrophy of the surrounding brain, have been reported in MEMRI images (30). More recently, Hsu et al. (31) verified signal hyperintensity in both CA1 and CA3 pyramidal cell layers after KA treatment. Our ROI measurement in the hippocampal area was also statistically significant in the KA-treated side of the rats.

Considering the present study and previous studies, we can conclude that MEMRI reflects local neuronal activation and is well correlated with histopathological changes in KA-induced hippocampal damage with neuropathology-related Mn^{2+} uptake (30, 31). The main limitation of the present study is the small number of animals. The lack of a specific area for animal handling in the MRI unit is a major problem for the overall reproducibility of these types of studies.

It is very important to have a dedicated high-field MRI unit with specially designed coils for small-animal studies despite their high cost (32). Many small-animal studies have been undertaken using clinical MRI systems with either commercial clinical coils or specific coils designed for small animals on 1.5 and 3 T MR units (32, 33). The major limitation of the use of an Mn²⁺-based contrast agent is cellular toxicity; thus, clinically, Mn²⁺-based contrast agents (Mn²⁺ dipyrithional diphosphate) have been developed with chelated Mn²⁺ (34). However, this contrast agent lacks the advantages of Mn²⁺ ions, which have the potential to detect various neurological disorders. Mn²⁺-based contrast agents have been used in many animal studies (34).

In conclusion, Mn²⁺-based contrast agents can be used to show neuronal damage in MRI experimentally. The development of an Mn²⁺-based contrast agent that can be safely used in humans is warranted to investigate neurological disorders.

Conflict of interest disclosure

The authors declared no conflicts of interest.

References

- Silva AC, Lee JH, Aoki I, Koretsky AP. Manganese-enhanced magnetic resonance imaging (MEMRI): methodological and practical considerations. *NMR Biomed* 2004; 17:532–543. [\[CrossRef\]](#)
- Pautler RG, Silva AC, Koretsky AP. In vivo neuronal tract tracing using manganese-enhanced magnetic resonance imaging. *Magn Reson Med* 1998; 40:740–748. [\[CrossRef\]](#)
- Massaad CA, Pautler RG. Manganese-enhanced magnetic resonance imaging (MEMRI). *Methods Mol Biol* 2011; 711:145–174. [\[CrossRef\]](#)
- Wang Q, Yu S, Simonyi A, Sun GY, Sun AY. Kainic acid-mediated excitotoxicity as a model for neurodegeneration. *Mol Neurobiol* 2005; 31:3–16. [\[CrossRef\]](#)
- Gruenthal M, Armstrong DR, Ault B, Nandler JV. Comparison of seizures and brain lesions produced by intracerebroventricular kainic acid and bicuculline methiodide. *Exp Neurol* 1986; 93:621–630. [\[CrossRef\]](#)
- Contractor A, Mülle C, Swanson GT. Kainate receptors coming of age: milestones of two decades of research. *Trends Neurosci* 2011; 34:154–163. [\[CrossRef\]](#)
- Shetty AK, Hattiangady B, Rao MS. Vulnerability of hippocampal GABA-ergic interneurons to kainate-induced excitotoxic injury during old age. *J Cell Mol Med* 2009; 13:2408–2423. [\[CrossRef\]](#)
- Silva AC, Bock NA. Manganese-enhanced MRI: an exceptional tool in translational neuroimaging. *Schizophr Bull* 2008; 34:595–604. [\[CrossRef\]](#)
- Cook AM, Mieure KD, Owen RD, Pesaturo AB, Hatton J. Intracerebroventricular administration of drugs. *Pharmacotherapy* 2009; 29:832–845. [\[CrossRef\]](#)
- Paxinos G, Watson C. The rat brain in stereotaxic coordinates, 6th ed. Amsterdam: Elsevier, 2007.
- Kjonigsen LJ, Leergaard TB, Witter MP, Bjaalie JG. Digital atlas of anatomical subdivisions and boundaries of the rat hippocampal region. *Front Neuroinform* 2011; 5:2. [\[CrossRef\]](#)
- Xiong N, Huang J, Zhang Z, et al. Stereotaxical infusion of rotenone: a reliable rodent model for Parkinson's disease. *PLoS One* 2009; 4:e7878. [\[CrossRef\]](#)
- Danscher G, Zimmer J. An improved Timm sulphide silver method for light and electron microscopic localization of heavy metals in biological tissues. *Histochemistry* 1978; 55:27–40. [\[CrossRef\]](#)
- Immonen RJ, Kharatishvili I, Sierra A, Einula C, Pitkänen A, Gröhn OH. Manganese-enhanced MRI detects mossy fiber sprouting rather than neurodegeneration, gliosis or seizure-activity in the epileptic rat hippocampus. *Neuroimage* 2008; 4:1718–1730. [\[CrossRef\]](#)
- Denic A, Macura SI, Mishra P, Gamez JD, Rodriguez M, Pirkó I. MRI in rodent models of brain disorders. *Neurotherapeutics* 2011; 8:3–18. [\[CrossRef\]](#)
- Dijkhuizen RM. Application of magnetic resonance imaging to study pathophysiology in brain disease models. *Methods Mol Med* 2006; 124:251–278.
- Hansen G, Crooks LE, Davis P, et al. In vivo imaging of the rat anatomy with nuclear magnetic resonance. *Radiology* 1980; 136:695–700.
- Meldrum BS. Glutamate as a neurotransmitter in the brain: review of physiology and pathology. *J Nutr* 2000; 130:1007–1015.
- Doble A. The role of excitotoxicity in neurodegenerative disease: implications for therapy. *Pharmacol Ther* 1999; 81:163–221. [\[CrossRef\]](#)
- Zhang XM, Zhu J. Kainic acid-induced neurotoxicity: targeting glial responses and glia-derived cytokines. *Curr Neuropharmacol* 2011; 9:388–398. [\[CrossRef\]](#)
- Byun JS, Lee SH, Jeon SH, et al. Kainic acid-induced neuronal death is attenuated by aminoguanidine but aggravated by L-NAME in mouse hippocampus. *Korean J Physiol Pharmacol* 2009; 13:265–271. [\[CrossRef\]](#)
- Pereno GL, Beltramino CA. Differential role of gonadal hormones on kainic acid-induced neurodegeneration in medial amygdaloid nucleus of female and male rats. *Neuroscience* 2009; 163:952–963. [\[CrossRef\]](#)
- Bardgett ME, Salaris SL, Jackson JL, Harding J, Csernansky JG. The effects of kainic acid lesions on dopaminergic responses to haloperidol and clozapine. *Psychopharmacology (Berl)* 1997; 133:142–151. [\[CrossRef\]](#)
- Nakai M, Qin ZH, Chen JF, Wang Y, Chase TN. Kainic acid-induced apoptosis in rat striatum is associated with nuclear factor-kappaB activation. *J Neurochem* 2000; 74:647–758. [\[CrossRef\]](#)
- Gillardot F, Wickert H, Zimmermann M. Up-regulation of bax and down-regulation of bcl-2 is associated with kainate-induced apoptosis in mouse brain. *Neurosci Lett* 1995; 192:85–88. [\[CrossRef\]](#)
- López E, Pozas E, Rivera R, Ferrer I. Bcl-2, Bax and Bcl-x expression following kainic acid administration at conversant doses in the rat. *Neuroscience* 1999; 91:1461–1470. [\[CrossRef\]](#)
- Henshall DC, Araki T, Schindler CK, et al. Activation of Bcl-2-associated death protein and counter-response of Akt within cell populations during seizure-induced neuronal death. *J Neurosci* 2002; 22:8458–8465.
- Cheung EC, Melanson-Drapeau L, Cregan SP, et al. Apoptosis-inducing factor is a key factor in neuronal cell death propagated by BAX-dependent and BAX-independent mechanisms. *J Neurosci* 2005; 25:1324–1334. [\[CrossRef\]](#)
- Uchino A, Noguchi T, Nomiyama K, et al. Manganese accumulation in the brain: MR imaging. *Neuroradiology* 2007; 49:715–720. [\[CrossRef\]](#)
- Nairismägi J, Pitkänen A, Narkilahti S, Huttunen J, Kauppinen RA, Gröhn OH. Manganese-enhanced magnetic resonance imaging of mossy fiber plasticity in vivo. *Neuroimage* 2006; 30:130–135. [\[CrossRef\]](#)
- Hsu YH, Lee WT, Chang C. Multiparametric MRI evaluation of kainic acid-induced neuronal activation in rat hippocampus. *Brain* 2007; 130:3124–3134. [\[CrossRef\]](#)
- Beuf O, Jaillon F, Saint-Jalmes H. Small-animal MRI: signal-to-noise ratio comparison at 7 and 1.5 T with multiple-animal acquisition strategies. *MAGMA* 2006; 19:202–208. [\[CrossRef\]](#)
- Pillai DR, Heidemann RM, Kumar P, et al. Comprehensive small animal imaging strategies on a clinical 3 T dedicated headMR-scanner; adapted methods and sequence protocols in CNS pathologies. *PLoS One* 2011; 6:e16091. [\[CrossRef\]](#)
- Van Meir V, Van der Linden A. Functional cellular imaging with manganese. In: Modo MM, Bulte JWM, eds. *Molecular and cellular MR imaging*. Boca Raton: CRC Press, 2007; 369–392. [\[CrossRef\]](#)